

## ORIGINAL RESEARCH

# Metabolomic exhibits different profiles and potential biomarkers of *Vitis* spp. co-cultivated with *Fusarium oxysporum* for short, medium, and long times

Igor Rafael Sousa Costa<sup>1</sup> | Francisco Lucas Pacheco Cavalcante<sup>1</sup> |  
 Fábio Rossi Cavalcanti<sup>2</sup> | Cleberson de Freitas Fernandes<sup>3</sup> | Enéas Gomes-Filho<sup>1</sup> |  
 Kirley Marques Canuto<sup>3</sup> | Humberto Henrique de Carvalho<sup>1</sup> 

<sup>1</sup>Department of Biochemistry and Molecular Biology, Sciences Center, Federal University of Ceará—Campus do Pici, Fortaleza, Brazil

<sup>2</sup>Empresa Brasileira de Pesquisa Agropecuária, Embrapa Uva e Vinho, Bento Gonçalves, Brazil

<sup>3</sup>Empresa Brasileira de Pesquisa Agropecuária, Embrapa Agroindústria Tropical, Fortaleza, Brazil

## Correspondence

Humberto Henrique de Carvalho, Department of Biochemistry and Molecular Biology, Sciences Center, Federal University of Ceará—Campus do Pici, CEP, 60440-554 Fortaleza, Ceará, Brazil.

Email: [humberto.carvalho@ufc.br](mailto:humberto.carvalho@ufc.br)

## Funding information

Conselho Nacional de Desenvolvimento Científico e Tecnológico, Grant/Award Numbers: 408118/2021-0, 306117/2022-3; Empresa Brasileira de Pesquisa Agropecuária, Grant/Award Number: SEG 22.16.04.035.00.00

Edited by H. Saitoh

## Abstract

Differential rootstock tolerance to *Fusarium* spp. supports viticulture worldwide. However, how plants stand against the fungus still needs to be explored. We hypothesize it involves a differential metabolite modulation. Thus, we performed a gas chromatography coupled with mass spectrometry (GC–MS) analysis of Paulsen P1103 and BDMG573 rootstocks, co-cultured with *Fusarium oxysporum* (FUS) for short, medium, and long time (0, 4, and 8 days after treatment [DAT]). In shoots, principal component analysis (PCA) showed a complete overlap between BDMG573 non-co-cultivated and FUS at 0 DAT, and P1103 treatments showed a slight overlap at both 4 and 8 DAT. In roots, PCA exhibited overlapping between BDMG573 treatments at 0 DAT, while P1103 treatments showed overlapping at 0 and 4 DAT. Further, there is a complete overlapping between BDMG573 and P1103 FUS profiles at 8 DAT. In shoots, 1,3-dihydroxyacetone at 0 and 4 DAT and maltose at 4 and 8 DAT were biomarkers for BDMG573. For P1103, glyceric acid, proline, and sorbitol stood out at 0, 4, and 8 DAT, respectively. In BDMG573 roots, the biomarkers were  $\beta$ -alanine at 0 DAT, cellobiose and sorbitol at both 4 and 8 DAT. While in P1103 roots, they were galactose at 0 and 4 DAT and 1,3-dihydroxyacetone at 8 DAT. Overall, there is an increase in amino acids, glycolysis, and tricarboxylic acid components in tolerant Paulsen P1103 shoots. Thus, it provides a new perspective on the primary metabolism of grapevine rootstocks to *F. oxysporum* that may contribute to strategies for genotype tolerance and early disease identification.

## 1 | INTRODUCTION

Grapevine (*Vitis* spp.) is a widespread fruit perennial plant of cultural and economic importance since grapes, leaves, and seeds are the basis for food, beverages, and medicinal products, among others (Venkitasamy et al., 2019). Like other plants, vines are susceptible to many trunk diseases, such as viruses, bacteria, and fungi, requiring intensive use of chemicals to limit the growth of these pathogens (Mondello et al., 2018). These products result in high costs and negative

economic and environmental impacts, which have led to the search for alternative management strategies and hybrids with higher resistance (Volynkin et al., 2021).

Several microorganisms provoke injury to plants, among them the soil fungus *Fusarium* spp., which are widely spread. It promotes vascular wilt, decline, and death in several important crops, such as banana (Zhang et al., 2019), melon (Sebastiani et al., 2017), tomatoes (Lagopodi et al., 2002), and grapevines (Brum et al., 2012; Revegla et al., 2018). On this way, *Fusarium oxysporum* Schl. f. sp. *herbemontis*

became a serious phytosanitary problem for viticulture in South Brazil (Vilvert et al., 2017). It mainly penetrates the grapevine's root tissues and colonizes the xylem, blocking water transport to leaves which can lead to plant death (Andrade et al., 1995; Grigolett-Júnior & Sonego, 1993; Ziedan et al., 2011). To control the invasion of microbial pathogens effectively, plants use preexisting physical resources and chemical barriers as well as inducible defence mechanisms that comprise a hypersensitive response, and systemic acquired resistance activated upon attack (Durrant & Dong, 2004). Indeed, *Fusarium oxysporum* (FUS), a necrotrophic pathogen, responds to root tissues injuries by triggering a defence mechanism that involves enzymatic induction, gene expressions, and metabolic alterations (Chen, Wu, et al., 2019; Van Loon et al., 2006). The use of resistant rootstocks is a long-term strategy to deal with biotic and abiotic stresses as they can tolerate adverse conditions (Cramer, 2010; Fraga et al., 2016). Among those genotypes are the traditional and widely recommended Paulsen 1103/P1103 (*Vitis berlandieri* × *Vitis rupestris*), characterized by its tolerance to *Fusarium* wilt, while others are still experimental, such as BDMG573/BM573 (*Vitis lambrusca* “Bordo” × *Vitis rotundifolia* “Magnólia”) due to known parental tolerance and rooting potential (Cavalcanti, 2021; Costa et al., 2010; Grigolett-Júnior & Sonego, 1993; Reinhart, 2013).

The study of those biochemical and molecular adjustments of the plant response to biotic stresses may provide insights that help to decode the mechanisms involved in a plant–microbe interaction (Wong et al., 2019; Xu et al., 2015). Likewise, the metabolite responses can be used as biomarkers to indicate the health status of plants and give information about the pathogenicity of eventual disease agents (Sankaran et al., 2010; Wong et al., 2020). In this regard, metabolomics may detect developmental changes in the plant metabolome, metabolite functions, and metabolic pathways affected by the stimulation of pathogenic fungi favouring the development of new strategies to control fungal diseases (Feussner & Polle, 2015; Nakabayashi & Saito, 2015; Tan et al., 2009). Certainly, the presence of the pathogen is quickly detected by tolerant plants, and metabolic signals are triggered to contain the infection. It results in changes in primary metabolism represented by a range of sugars, amino acids, and organic acids. In general, there are changes in the source–drain relations due to high-energy demand, which promotes the availability of monosaccharides such as glucose and fructose (Gupta et al., 2010).

Metabolomics based on gas chromatography coupled to mass spectrometry (GC–MS) is a large-scale analytical technique used to study several metabolites simultaneously in a complex mix of biological extracts. It has high robustness, reproducibility, sensitivity, and low cost (Alseekh et al., 2021; Beale et al., 2018). In the last decade, metabolomics techniques helped study plant–pathogen fungal interactions to clarify the mechanisms triggered in the host that help the plant defence (Chen, Ma, & Chen, 2019). Indeed, GC–MS identified the increase of primary metabolites in chickpea and common bean upon FUS infection, in which amino acids and sugars act as energy or signalling molecules with a role in innate defence pathways (Chen, Wu, et al., 2019; Gupta et al., 2010). Metabolites such as arginine, aspartic acid, histidine, valine, and lysine were described for monitoring the

disease in watermelon plants (Kasote et al., 2020). Thus, metabolic profiles of grapevine with *Fusarium* vascular wilt may range according to genotypes and tissues.

The main goal of this work was to study primary metabolism in the plant–pathogen interaction of two grapevine genotypes, with tissue sampling based on a method by Cavalcanti (2021), challenged by *F. oxysporum* Schl. f. sp. *herbemontis* isolates using a GC–MS-based metabolomic approach. Plant/fungus co-cultivation under in vitro conditions induced primary metabolite modulation as one of the responses caused by vine trunk pathogens in the first stages of their parasitism. Therefore, this work provides a discussion of primary metabolite profile modulation of two rootstocks induced by short (0 days after treatment [DAT]), medium (4 DAT), and long (8 DAT) fungal infection. Thus, identifying potential markers that can be used to monitor or diagnose the disease at different times and to assist in breeding programs to reduce the alarming losses of viticulture caused by *Fusarium* worldwide.

## 2 | MATERIALS AND METHODS

### 2.1 | Chemicals

GC-grade *n*-Hexane and methanol were used to extract and obtain polar fractions of analytical interest. Carbohydrates, amino acids, organic acids, and ribitol used as standards have 99.0% purity. Methoxyamine hydrochloride, pyridine, and *N*-methyl-*N*-(trimethylsilyl) trifluoro-acetamide were used for gas chromatography derivatization step. All HPLC-grade chemicals were purchased from Merck Sigma-Aldrich.

### 2.2 | Plant and fungal materials

The biological materials were produced as previously reported (Cavalcanti, 2021). The seedling clones were provided by the laboratory of Vegetal Propagation of Embrapa Uva e Vinho located in Bento Gonçalves (Rio Grande do Sul State, Brazil) corresponding to the following *Vitis* spp. rootstocks: BDMG573 (Bordó [*V. labrusca*] × Magnólia [*V. rotundifolia*]) and “Paulsen” (P1103) (*V. berlandieri* × *V. rupestris*; Figure S1). They were grown in a culture containing a solid Galzy medium (Tanaka et al., 2001) until they reached 60 days. Briefly, approximately 3 cm diameter nodal segments with an axillary bud and a leaf were cut from plants and were cultured in new tubes containing 12 mL of medium supplemented with 8.0 μmol L<sup>-1</sup> naphthaleneacetic acid, 2% sucrose and 0.6% agar, pH 6.1, and autoclaved at 1 atm and 121°C for 20 min. The regenerated seedlings were propagated in vitro in duplicates, in culture tubes (11.5 × 2.5 cm) with approximately 5 mL of medium and kept in a growth chamber at 23 ± 3°C, under a photoperiod of 16 h with PPFD of 75 μmol photons m<sup>-2</sup> s<sup>-1</sup>. After rooting (45–60 days), one seedling was transferred into a new Galzy medium tube under the same conditions described earlier. The *F. oxysporum* Schl. f. sp. *herbemontis* colonies were established in an agar-based

medium for two weeks provided by the Laboratory of Phytopathology of Embrapa Agroindústria Tropical located in Fortaleza (Ceará State, Brazil). The co-cultured lineage experienced in trials was the strain “BRM004941” (<https://www.ncbi.nlm.nih.gov/nuccore/MG461601.1>) isolated from the trunk of “Seibel” vine and recorded at the microorganism collection of Embrapa Uva e Vinho (CMIA, Bento Gonçalves/RS, Brazil).

### 2.3 | Experimental and co-cultivation conditions and treatments

*In vitro*, co-cultivation was performed in a sterilized laminar flow hood by transferring 3 mm disks of potato dextrose agar with fungal mycelia into each tube containing the seedling (2 mm away from the stem) using sterile forceps (Cavalcanti, 2021). Then, the tubes were closed, sealed with plastic film, and placed in an acclimatized room at 25°C for a 12 h photoperiod. For the control group (non-co-cultivated [CNT]), the tubes containing the seedlings in the Galzy medium were not exposed to any fungus colonies and were kept in the same conditions as the co-cultured FUS group. The seedlings were evaluated at three different times after treatment (days after treatment [DAT]) with the fungus: (1) day “zero,” which was at 8 h after treatment (0 DAT); (2) after 4 days of treatment (4 DAT); and (3) after 8 days of treatment (8 DAT). The co-cultured and control groups were collected at the times described earlier. Their roots were separated from the aerial parts and immediately placed in liquid N<sub>2</sub> and stored at –80°C in an ultra-freezer. Thus, the experiment consisted of two *Vitis* spp. rootstock genotypes, BDMG573 and Paulsen P1103, two treatments, CNT and FUS, and three harvest times (0, 4, and 8 DAT), comprising four biological replicates.

### 2.4 | Plant extract preparation

To obtain the plant extract, the aerial part and roots were initially powdered in liquid N<sub>2</sub>. Afterwards, 50 mg of each plant material was mixed with 4 mL of hexane, vortexed for 1 min to homogenize, and placed in an ultrasound bath at 135 W for 20 min. Next, 4 mL of a methanol/water (7:3) solution was added to the mixture, repeating the vortex and ultrasonic bath steps. The solution was centrifuged at 12,000 g for 10 min, yielding two phases (nonpolar and polar supernatant). Finally, 1.0 mL aliquots of the lower phase (water–methanol) were filtered through hydrophilic Polytetrafluoroethylene 0.22 µm filter and stored in vials at –80°C until GC–MS analysis. A 250 µL aliquot of the water–methanol (polar) phase was mixed with 30 µL of the internal standard ribitol (0.2 mg mL<sup>–1</sup>) and centrifuged at 12,000 g for 10 min. Later, an aliquot of 250 µL of the supernatant was transferred to a microtube and dried in a speed vac equipment (SpeedVac Concentrator, Eppendorf) overnight. Finally, the metabolites from the dry polar fractions were derivatized using methoxylamine hydrochloride (20 mg mL<sup>–1</sup>) in pyridine by shaking at 37°C for 2 h, followed by addition of

*N*-methyl-*N*-(trimethylsilyl)-trifluoro acetamide. The reaction mixture was kept under stirring at 37°C for 30 min and injected in the GC–MS (Lisec et al., 2006).

### 2.5 | Gas chromatography and mass spectrometry conditions

The GC–MS analyses were done on a QP–PLUS 2010 Shimadzu GC–MS instrument. One microliter sample was injected in split mode (1:10 ratio) with helium gas as carrier gas at a flow rate of 1.0 mL min<sup>–1</sup> in an RTX-5MS capillary column (30 mm × 0.25 mm × 0.25 µm) to separate the metabolites. The chromatographic runs were carried out in four replicates at 80°C for 5 min, then increased to 310°C by 8°C min<sup>–1</sup> and maintained for 1 min at this temperature. The injection, ions source, and MS interface temperatures were 230, 200, and 250°C, respectively. The mass spectrometer was operated at 70 eV (EI) in a scanning range of 80–700 (m/z), initiated after a solvent cut-off time of 3.5 min. The chromatograms and mass spectra were processed using the Xcalibur™ 2.1 software (Thermo Fisher Scientific). The metabolites were identified based on the comparison of their retention times and fragmentation patterns of amino acids, carbohydrates, and organic acids previously obtained (Batista et al., 2019; Lima et al., 2022), an internal MS library composed of metabolite standards and as well with those of Golm's metabolome database Arabidopsis fragmentation patterns (Max Planck Institute of Molecular Plant Physiology) available in <http://gmd.mpimp-golm.mpg.de/analysisinput.aspx>. The relative value of each metabolite was determined by dividing their respective peak areas by the internal standard ribitol peak area, then divided by the fresh mass of the sample. Then, metabolites were identified and classified using the Kyoto Gene and Genome Encyclopedia (KEGG) database.

### 2.6 | Experimental design and statistical analysis

The experimental design consisted of two *Vitis* spp. rootstock genotypes, two treatments (CNT and FUS) at three DATs (0, 4, and 8). For the metabolic analysis, the files were processed on the MetaboAnalyst 5.0 server (<http://www.metaboanalyst.ca>) web-based interface. The data were normalized by log transformation (base 10) and automatic scaling (mean-centered and divided by the standard deviation of each variable) that fitted a better statistical normal distribution. The principal component analysis (PCA) was performed to show the differences between the two treatments and analyzed times for each plant tissue separately. To evaluate the effect of the treatment concerning the control on the metabolic profile, orthogonal partial least squares analysis-discriminant analysis (OPLS-DA) and variable importance in projections (VIP scores) were performed for leaves and roots separately for each genotype and times, obtaining the principal discriminating metabolites. The hierarchical heatmaps were built by Euclidean distance based on a one-way analysis of variance (ANOVA).

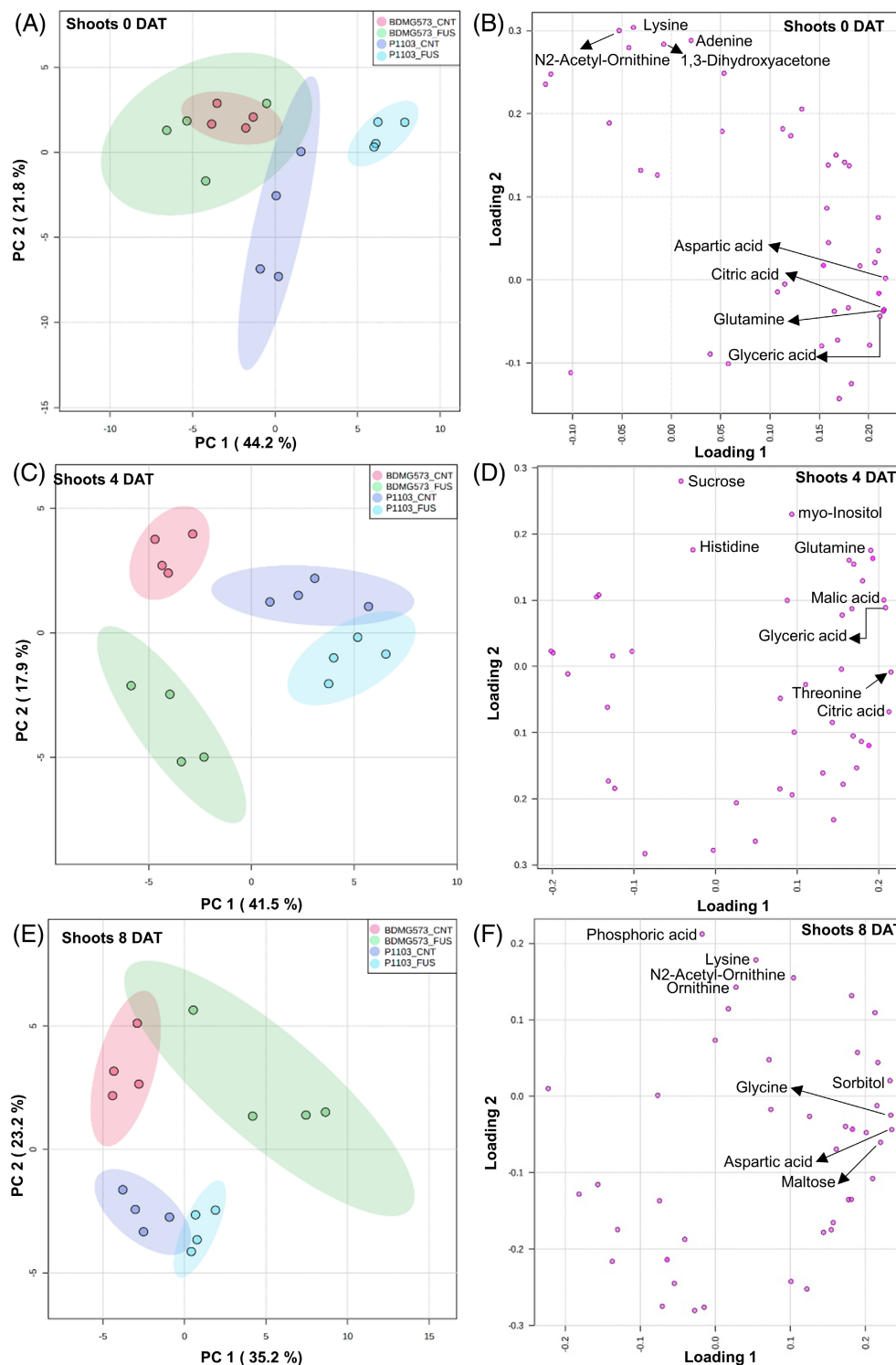
**TABLE 1** List of metabolites detected in both BDMG573 and P1103, as well as roots and shoots.

Metabolites	Compound type	Retention time (min)	Compound id
Lactic acid	Organic acid	7.38	C00186
Alanine	Amino acids	8.43	C00041
1,3-Dihydroxyacetone	Carbohydrates	10.23	C00184
Valine	Amino acids	11.01	C00183
Urea	Others	11.43	C00086
Serine	Amino acids	11.83	C00065
Leucine	Amino acids	12.15	C01933
Phosphoric acid	Organic acid	12.23	C00009
Glycerol	Carbohydrates	12.24	C00116
Isoleucine	Amino acids	12.57	C00407
Proline	Amino acids	12.61	C00148
Glycine	Amino acids	12.81	C00037
Glyceric acid	Organic acid	13.32	C00258
Fumaric acid	Organic acid	13.49	C00122
Maleic acid	Organic acid	13.51	C01384
Threonine	Amino acids	14.33	C00188
$\beta$ -Alanine <sup>a</sup>	Amino acids	14.93	C00099
Malic acid	Organic acid	16.02	C00149
Methionine	Amino acids	16.46	C00073
Aspartic acid	Amino acids	16.51	C00049
4-hydroxy-proline	Amino acids	16.61	C03651
N-acetyl-Serine	Amino acids	17.63	C00979
Asparagine	Amino acids	17.88	C00152
Glutamic acid	Amino acids	17.98	C00025
Phenylalanine	Amino acids	18.11	C00079
Xylose	Carbohydrates	18.71	C00181
Arabinose	Carbohydrates	18.77	C00216
Ribose	Carbohydrates	19.01	C00121
Glutamine	Amino acids	20.16	C00064
Ornithine	Amino acids	20.76	C00077
Citric acid	Organic acid	20.85	C00158
Adenine	Others	21.41	C00147
Fructose	Carbohydrates	21.77	C02336
Mannose	Carbohydrates	21.82	C00159
Glucose	Carbohydrates	21.98	C00031
Lysine	Amino acids	22.06	C00047
N <sub>2</sub> -acetyl-Ornithine	Amino acids	22.07	C00437
Histidine	Amino acids	22.12	C00135
Galactose	Carbohydrates	22.18	C00124
Tyrosine	Amino acids	22.3	C00082
Sorbitol	Carbohydrates	22.37	C00794
Glucuronic acid	Carbohydrates	22.48	C16245
Inositol-myo	Carbohydrates	24.28	C00137
Sucrose	Carbohydrates	30.03	C00089
Cellobiose	Carbohydrates	30.98	C06422
Maltose	Carbohydrates	31.27	C00208

Note: The names and compound IDs were based on the Kyoto Encyclopedia of Genes and Genomes (KEGG ID).

<sup>a</sup> $\beta$ -alanine was found only in roots.

**FIGURE 1** Two-dimensional principal component analysis (PCA) of shoots metabolic profiles of two *Vitis* spp. genotypes BDMG573 and P1103. The plants were co-cultivated with *Fusarium oxysporum* (FUS) or non-co-cultivated (CNT) and evaluated at 8 h or 0 days after treatment (DAT) (A), 4 DAT (C), and 8 DAT (E). The loading plots indicate each metabolite contribution for distribution of groups at 0 DAT (B), 4 DAT (D), and 8 DAT (F). Arrows indicated the most top four positive metabolites that were named. The ellipses indicate a 95% confidence interval of the group.



### 3 | RESULTS

#### 3.1 | Metabolic profiles of two *Vitis* spp. rootstocks during different lengths of *Fusarium* infection

A previous comparison of the rootstocks Paulsen P1103 and BDMG573 co-cultivated with FUS demonstrated that after 4 days,

the percentage of infection increased more in BDMG573 than in P1103 since the progress of infection in P1103 was delayed. Thus we decided to evaluate the metabolite modulation of 0, 4, and 8 days of co-cultivation (Cavalcanti, 2021).

A total of 46 metabolites were identified of which 22 were amino acids, 7 were organic acids, 15 were carbohydrates, and 2 belonged to other classes (Table 1). The classification was based on the KEGG ID, the retention times, and mass fragmentation pattern.

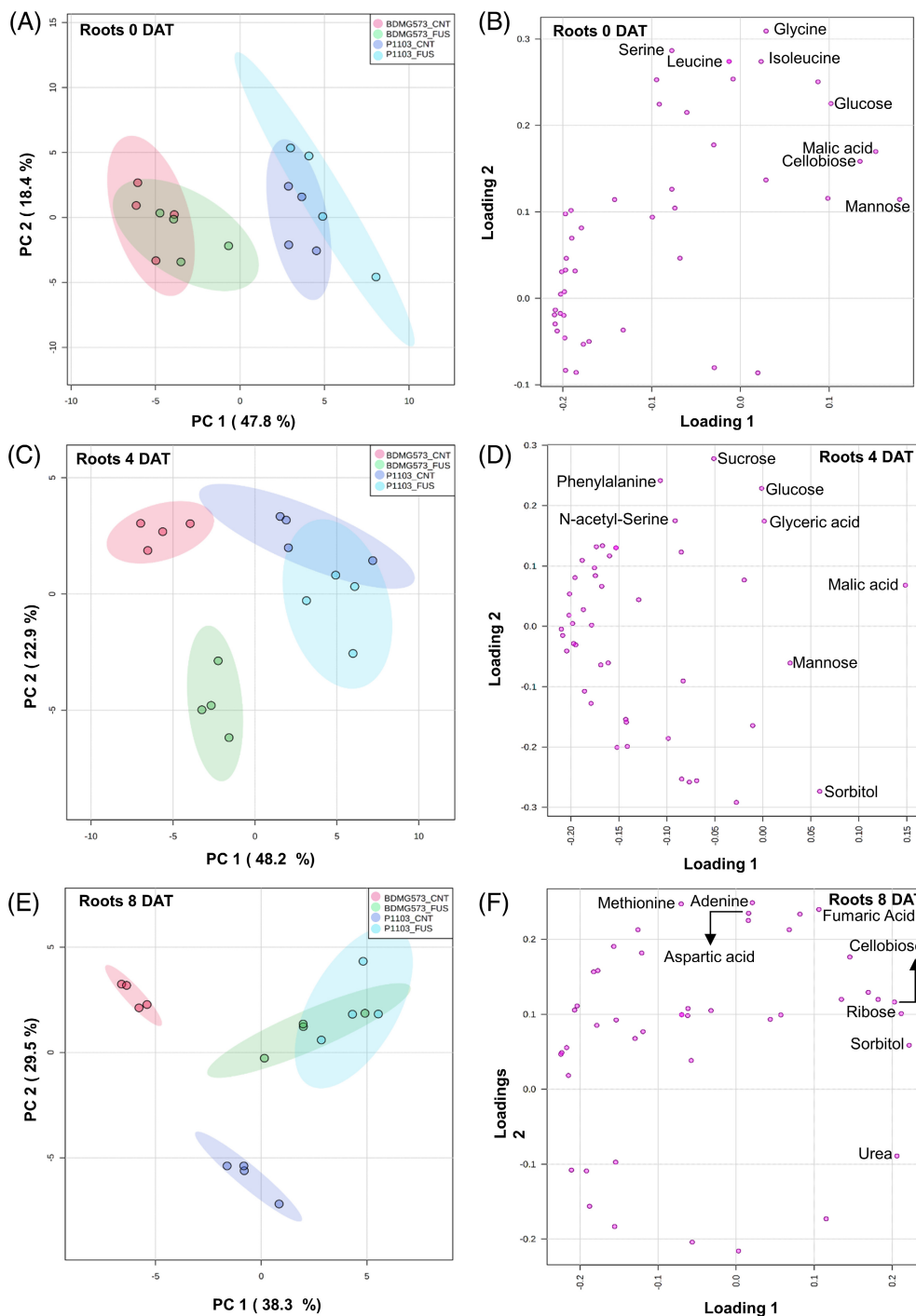


**FIGURE 2** Two-dimensional principal component analysis (PCA) of roots metabolic profiles of two *Vitis* spp. genotypes BDMG573 and P1103. The plants were co-cultivated with *Fusarium oxysporum* (FUS) or non-co-cultivated (CNT) and evaluated at 8 h or 0 days after treatment (DAT) (A), 4 DAT (C), and 8 DAT (E). The loading plots indicate each metabolite contribution for distribution of groups at 0 DAT (B), 4 DAT (D), and 8 DAT (F). Arrows indicated the most top four positive metabolites that were named. The ellipses indicate a 95% confidence interval of the group.

Forty-five metabolites were found in shoots of both genotypes, and 46 were found in the roots.  $\beta$ -Alanine was present only in the roots.

To evaluate differences between control CNT and co-cultivated with the FUS of both genotypes after different lengths of treatment (0 DAT, 4 DAT, and 8 DAT), we performed multivariate analyses of principal component (PC) of the GC-MS dataset from shoots and roots, separately. Considering shoot, at 0 DAT, the PC1 and PC2 accounted for 44.2% and 21.8% of the total variation, respectively (Figure 1A). The plot showed a complete separation of P1103\_FUS

from the other treatments influenced mainly by the PC1 component. On the other hand, there was a complete overlap between BDMG573\_CNT and BDMG573\_FUS, indicating similar metabolic profiles, besides there is an overlapping between the confidence intervals of BDMG573\_FUS and P1103\_CNT. The top four positive contributions to PC1 were aspartic acid, citric acid, glutamine, and glyceric acid, and to PC2 lysine,  $N_2$ -Acetyl-ornithine, and adenine (Figure 1B). All metabolite contributions have been provided (Table S1). At 4 DAT, the PC1 and PC2 accounted for 41.5% and 17.9% of the total variation, respectively (Figure 1C). The scores plot exhibited a clear

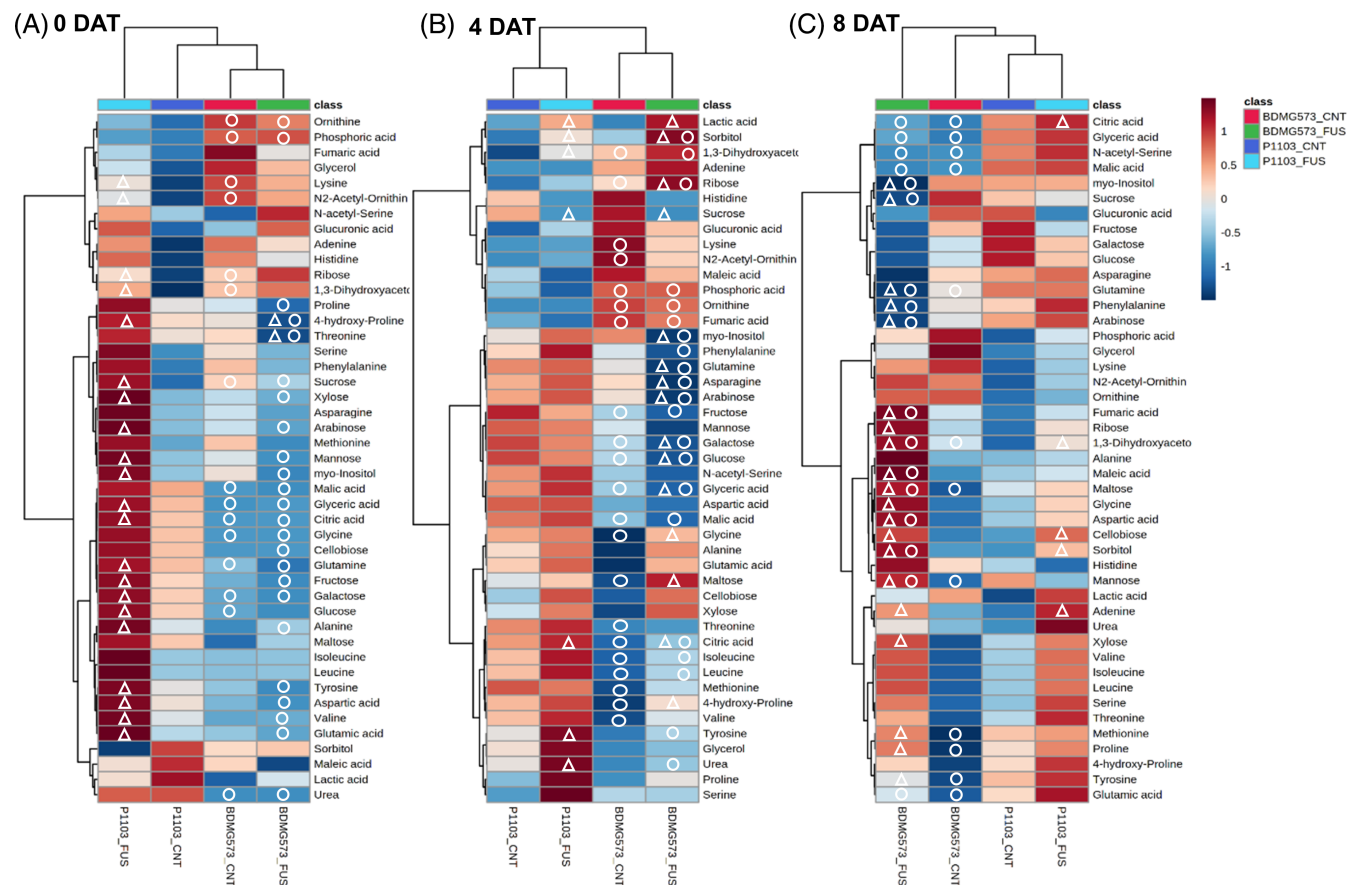


**FIGURE 3** Hierarchical heat maps grouped by Euclidean distance of shoots genotypes P1103 and BDMG573 at different times of co-culture with *Fusarium oxysporum* (FUS), as well as the control non-co-cultured (CNT). (A) 0 days after treatment (DAT), (B) 4 DAT, and (C) 8 DAT. The squares represent the  $\log_2$  mean of four replicates, and the color map shows an increase (red scale) or decrease (blue scale) of each metabolite. Triangles indicate significant difference by ANOVA ( $p < 0.05$ ) between treatments within the same genotype (BDMG573\_FUS  $\times$  BDMG573\_CNT or P1103\_FUS  $\times$  P1103\_CNT). Circles indicate significant difference between genotypes within the same treatment (BDMG573\_FUS  $\times$  P1103\_FUS or BDMG573\_CNT  $\times$  P1103\_CNT).

separation among the four treatments. The top four metabolites that contributed to groups separation were threonine, citric acid, glyceric acid, and malic acid for PC1, and sucrose, myo-inositol, histidine, and glutamine for PC2 (Figure 1D; Table S1). At 8 DAT, the PC1 and PC2 accounted for 35.2% and 23.2% of the variation, respectively (Figure 1E). There was a well-defined separation between BDMG573 and P1103, independent of the treatment influenced by the PC2 axis. Although there was a broad distribution of BDMG573\_FUS over the plot, it overlapped the BDMG573\_CNT, and the P1103\_CNT confidence interval overlapped with P1103\_FUS as well. The top four metabolites contributing to group the discrimination were aspartic acid, glycine, sorbitol, and maltose for PC1, followed by phosphoric acid, lysine, N<sub>2</sub>-acetyl-ornithine, and ornithine for PC2 (Figure 1F; Table S1).

Similarly, PCA evaluated the root metabolites of both genotypes for each time point. At 0 DAT, PC1 and PC2 accounted for 47.5% and 18.4% of the total variation, respectively (Figure 2A). The PCA plots exhibited a well-defined separation between the BDMG573 and P1103 genotypes by PC1 axis. However, there were overlaps between BDMG573\_CNT and BDMG\_FUS and between P1103\_CNT and P1103\_FUS, indicating a similar metabolic profile for each

genotype under CNT and FUS treatments. The top four positive contributions were mannose, malic acid, cellobiose, and glucose for PC1, followed by glycine, serine, leucine, and isoleucine for PC2 (Figure 2B; Table S2). At 4 DAT, the PC1 and PC2 accounted for 48.2% and 22.9% of the total variation, respectively (Figure 2C). The plot exhibited a well-defined separation between the BDMG573 and P1103 genotypes and between the BDMG573\_CNT and BDMG573\_FUS treatments, indicating a higher variation in BDMG573 at 0 DAT. On the other hand, there was an overlap between P1103 treatments, as noticed at 0 DAT. The top four metabolites that contributed to groups separation were malic acid, sorbitol, mannose, and glyceric acid for PC1, and sucrose, phenylalanine, glucose, and N-acetyl-serine for PC2 (Figure 2D; Table S2). At 8 DAT, the PC1 and PC2 accounted for 38.3% and 29.5% of the variation, respectively (Figure 2E). There was a well-defined separation between BDMG573\_CNT and P1103\_CNT, and they separated from their respective FUS treatment. On the other hand, the profile of BDMG573\_FUS overlapped with P1103\_FUS. The top four metabolites contributing to the group separation were sorbitol, ribose, urea, and cellobiose for PC1, followed by adenine, methionine, fumaric acid, and aspartic acid for PC2 (Figure 2F; Table S2).

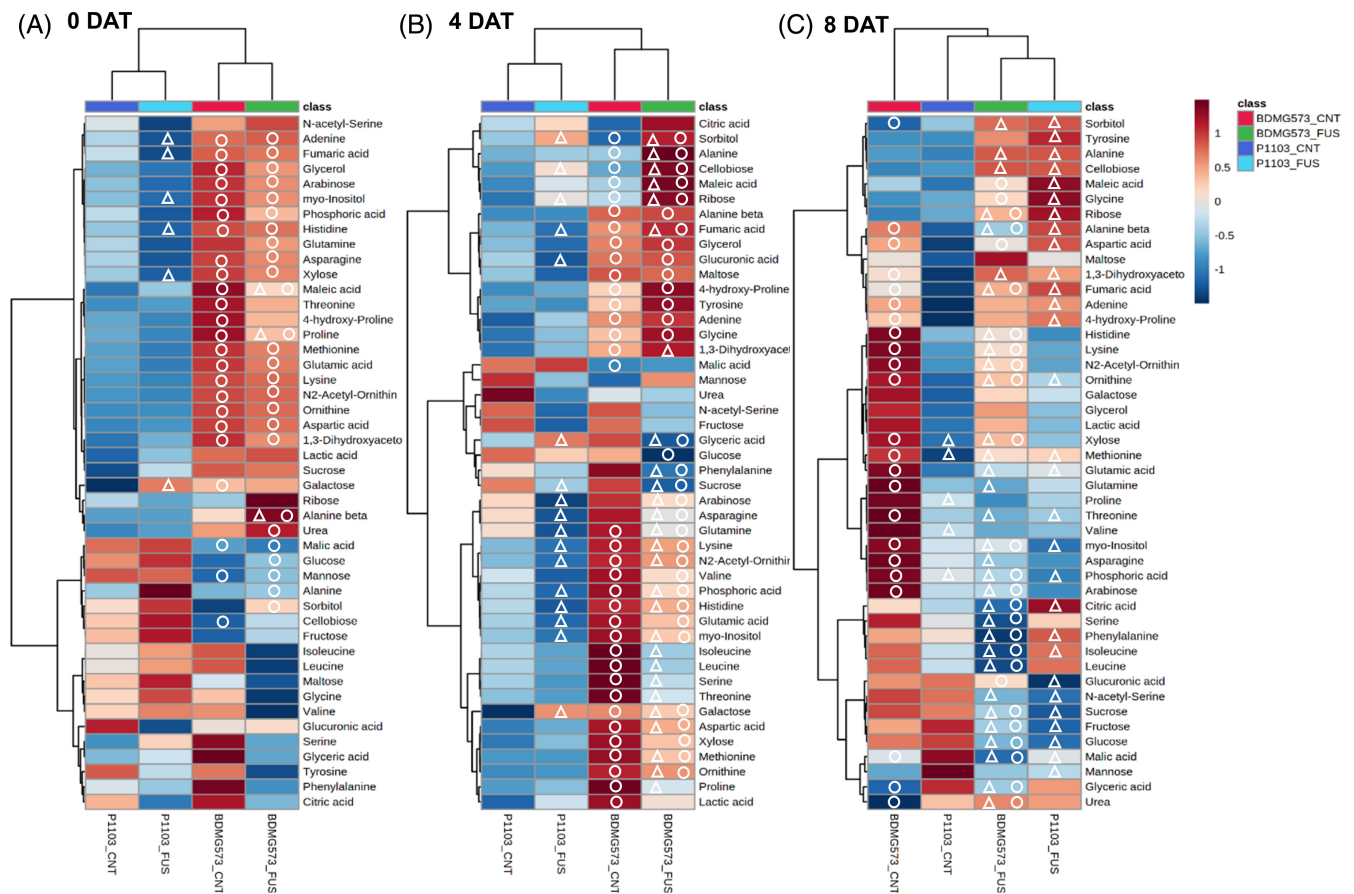


**FIGURE 4** Hierarchical heat maps grouped by Euclidean distance of roots genotypes P1103 and BDMG573 at different times of co-culture with *Fusarium oxysporum* (FUS), as well as the control non-co-cultured (CNT). (A) 0 days after treatment (DAT), (B) 4 DAT, and (C) 8 DAT. The squares represent the log<sub>2</sub> mean of four replicates, and the color map shows an increase (red scale) or decrease (blue scale) of each metabolite. Triangles indicate significant difference by ANOVA ( $p < 0.05$ ) between treatments within the same genotype (BDMG573\_FUS  $\times$  BDMG573\_CNT or P1103\_FUS  $\times$  P1103\_CNT). Circles indicate significant difference between genotypes within the same treatment (BDMG573\_FUS  $\times$  P1103\_FUS or BDMG573\_CNT  $\times$  P1103\_CNT).

### 3.2 | Identification of significant metabolite modulation in *Vitis* spp. rootstocks during *Fusarium* infection

Heat maps detailing the positive or negative modulation of metabolites were generated comprising the two genotypes (BDMG573 and P1103) of each treatment separately by DAT, similar to the PCA. The metabolites with statistical differences ( $p < 0.05$ ) were identified between the comparisons: BDMG573\_CNT/BDMG573\_FUS, P1103\_CNT/P1103\_FUS, as well as BDMG573\_CNT/P1103\_CNT, and BDMG573\_FUS/P1103\_FUS. The analysis of the shoot heatmaps showed a division between the FUS and CNT treatments in the BDMG573 genotype at 0 and 4 DAT. While in the P1103 genotype, the division occurred at 4 and 8 DAT (Figure 3). At 0 DAT, only two metabolites (4-hydroxyproline and threonine) were significantly different between BDMG573\_FUS and CNT. However, 21 metabolites were significantly different in P1103\_FUS compared to control, most of which had a positive modulation. Comparing the different genotypes with the same treatment, 15 and 25 metabolites were significantly

different between BDMG573\_CNT and P1103\_CNT and BDMG573\_FUS and P1103\_FUS (Figure 3A). At 4 DAT, there were 15 metabolites significantly modulated between BDMG573\_FUS and CNT, positively and negatively, whereas only seven metabolites were significantly altered in P1103\_FUS compared to control. Comparing the genotypes, 21 and 22 metabolites were different when treated the same, BDMG573\_CNT and P1103\_CNT and BDMG573\_FUS and P1103\_FUS (Figure 3B). At 8 DAT, there were 20 metabolites significantly modulated between BDMG573\_FUS and CNT (five increased, and 15 decreased), whereas only five metabolites were significantly increased in P1103\_FUS compared to control. Comparing different genotypes, 12 and 20 metabolites were significant between treatments BDMG573\_CNT and P1103\_CNT and BDMG573\_FUS and P1103\_FUS (Figure 3C).

Regarding the heatmaps of roots, there are six (in which five were increased and one was decreased) metabolites in P1103\_FUS and three decreased metabolites in the BDMG573\_FUS statistically different when compared to their control treatments at 0 DAT (Figure 4A). Overall, the heatmap showed that several metabolites were higher in

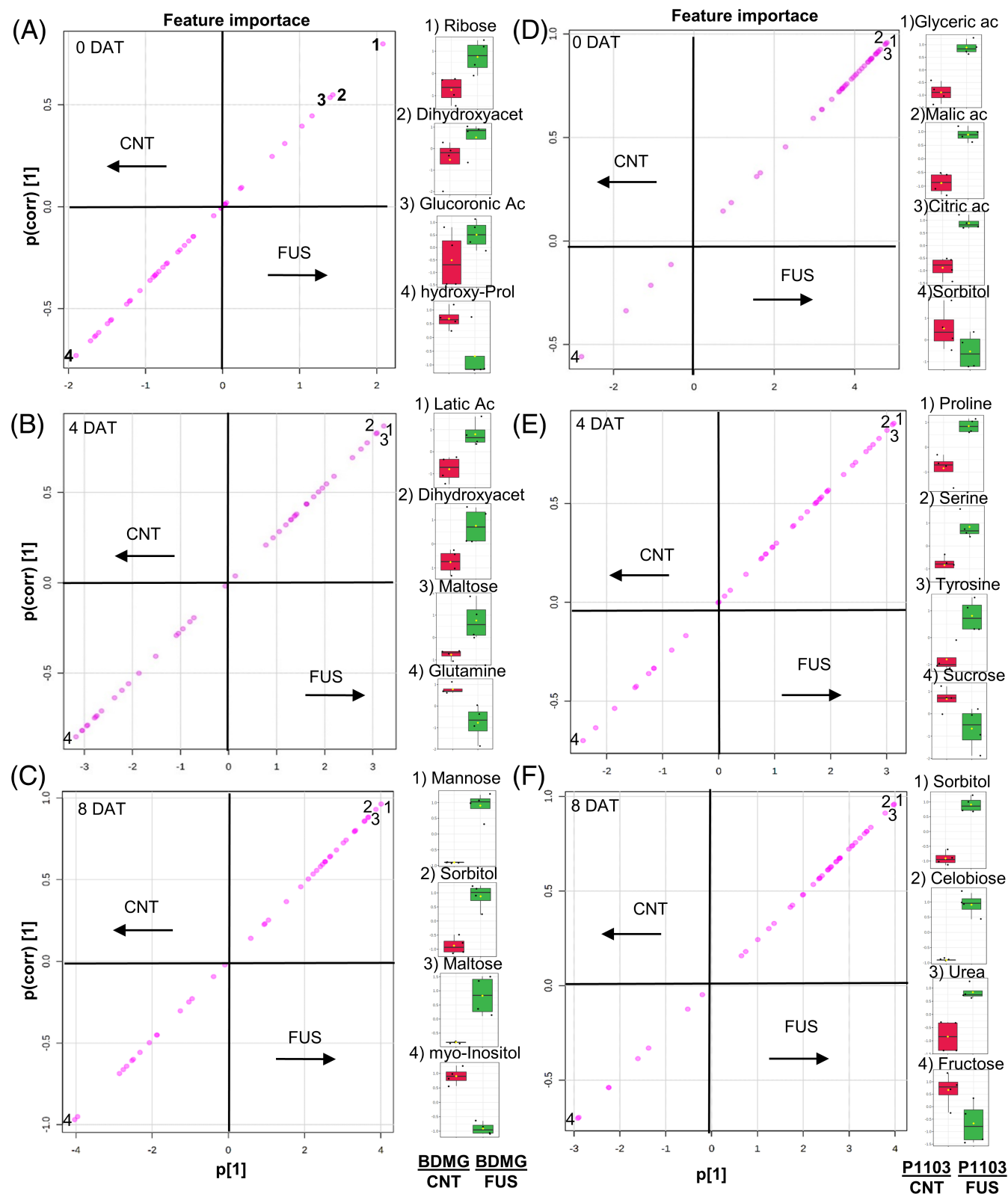


**FIGURE 5** S-plots from orthogonal projections to latent structures discriminant analysis (OPLS-DA) in shoots of *Vitis* spp. genotypes BDMG573 (A, B, and C) and P1103 (D, E, and F) co-cultured with *Fusarium oxysporum* fungus (FUS) compared to non-co-cultivated (CNT). The three most significant metabolites that had the major contribution to FUS (upper right corner) and CNT seedlings (lower left corner) were highlighted and their relative content were provided on the right of each plot.

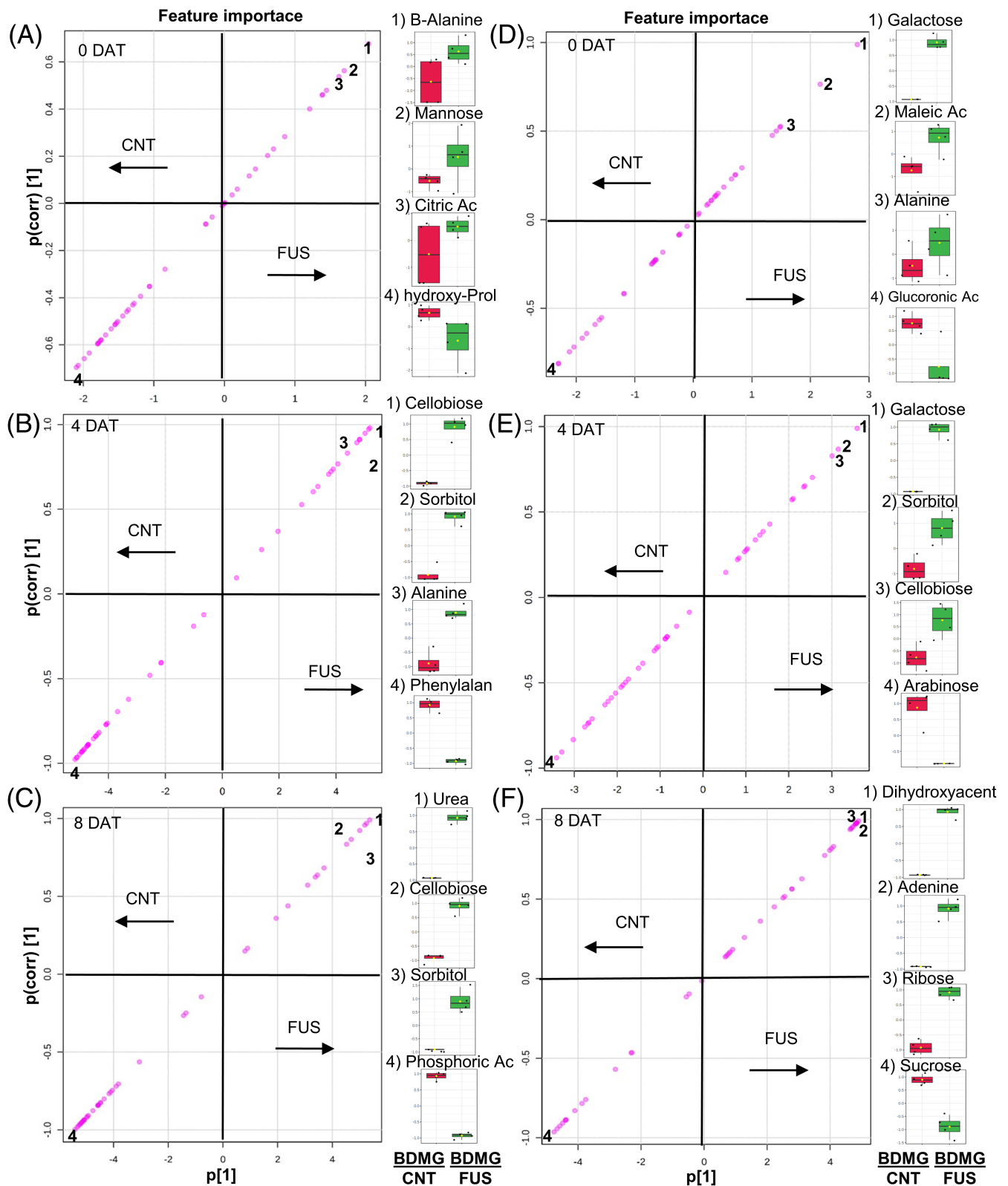


**FIGURE 6** S-plots from orthogonal projections to latent structures discriminant analysis (OPLS-DA) roots of *Vitis* spp. genotypes BDMG573 (A, B, and C) and P1103 (D, E, and F) co-cultured with *Fusarium oxysporum* fungus (FUS) compared to non-co-cultivated (CNT). The three most significant metabolites that had the major contribution to FUS (upper right corner) and CNT seedlings (lower left corner) were highlighted and their relative content were provided on the right of each plot.

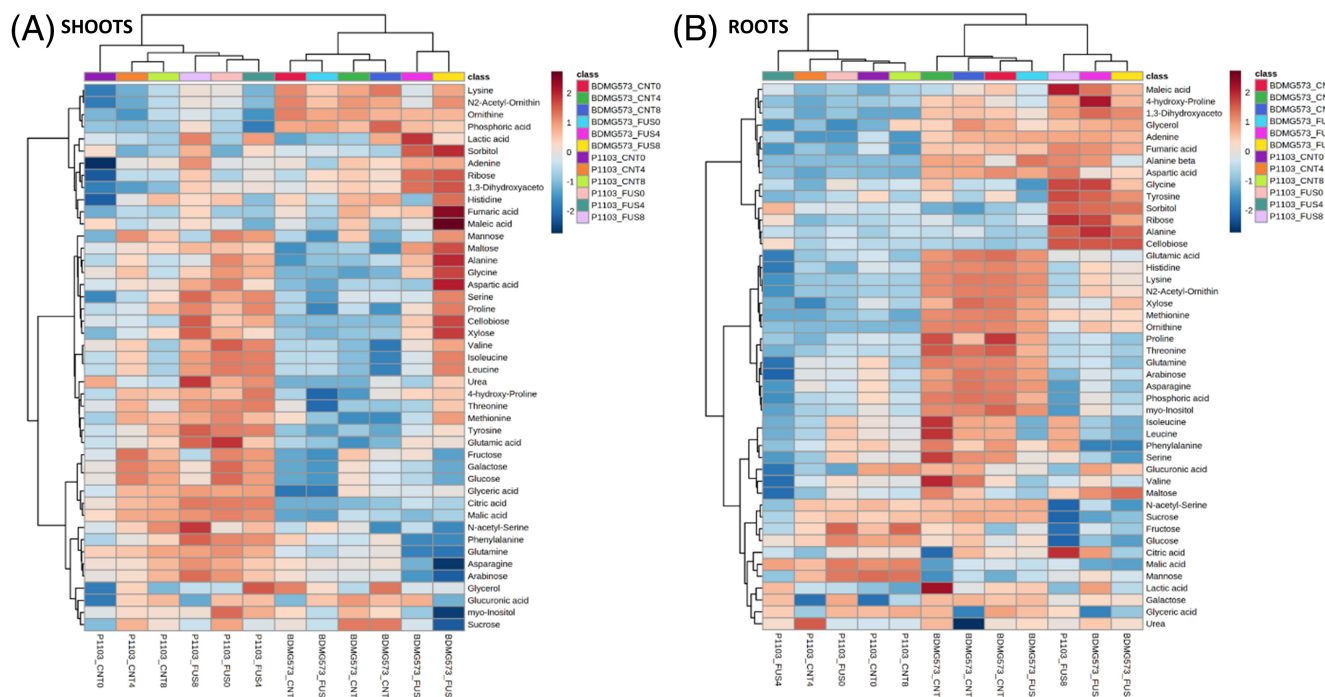


**FIGURE 7** Hierarchical heat maps grouped by Euclidean distance of shoots (A) and roots (B) metabolites of the two varieties of *Vitis* spp. BDMG573 and P1103. Each square represents the  $\log_2$  mean of four replicates, and the colour map shows an increase (red scale) or decrease (blue scale) of each metabolite compared to the control and co-cultivated plants for each time point (0, 4, and 8 days after treatment [DAT]). CNT, non-co-cultivated; FUS, *Fusarium oxysporum*.

the BDMG genotype. There were 24 and 25 metabolites differentially modulated when comparing the two genotypes in each treatment, respectively, BDMG573\_CNT  $\times$  P1103\_CNT and BDMG573\_FUS  $\times$  P1103\_FUS (Figure 4A). At 4 DAT, 28 and 16 were significantly modulated in the genotypes BDMG573\_FUS and P1103\_FUS, respectively (Figure 4B). Among them, a large number of amino acids decreased in both genotypes, while some sugars were increased while others were decreased. Comparing the genotypes in each treatment, BDMG573\_CNT  $\times$  P1103\_CNT and BDMG573\_FUS  $\times$  P1103\_FUS, 31 and 30 metabolites were differentially modulated, respectively. At 8 DAT, there were 32 (seven most positive, highlighting alanine, cellobiose, and 1,3-dihydroxyacetone) and 26 metabolites significantly modulated in genotypes BDMG573\_FUS and P1103\_FUS, respectively (Figure 4C). On the other hand, 17 and 23 metabolites were statistically different when comparing BDMG573\_CNT  $\times$  P1103\_CNT and BDMG573\_FUS  $\times$  P1103\_FUS, respectively.

### 3.3 | Potential biomarkers of FUS co-cultivation

OPLS-DA exhibited the positive and negative potential biomarkers of each *Vitis* spp. genotype co-cultivated with FUS at three different times (Table S3). We explored the S-plot since it combines the contribution of probability and correlation ranked from the highest to the lowest reliability values using the respective control treatment (CNT) as a reference. Analyzing the shoots of BDMG573\_FUS compared to

the control treatment, the top three positive metabolites were ribose, 1,3-dihydroxyacetone, and glucuronic acid, and 4-hydroxy-proline was the most negative at 0 DAT (Figure 5A). At 4 DAT, the three positive metabolites were lactic acid, 1,3-dihydroxyacetone, and maltose, and glutamine was the most negative (Figure 5B). At 8 DAT, the three positive metabolites were mannose, sorbitol, and maltose; myo-inositol was the most negative (Figure 5C). The same was performed for shoots of P1103\_FUS compared to the control treatment. At 0 DAT, the top three positive metabolites were glyceric, malic, and citric. The sugar sorbitol had the most negative influence (Figure 5D). At 4 DAT, the three positive discriminant metabolites were proline, serine, and tyrosine. Sucrose had the most negative impact (Figure 5E). At 8 DAT, sorbitol, cellobiose, and urea were the three positive metabolites. Fructose was the most negative (Figure 5F). The variable importance of metabolites in projections (VIP scores) with VIP >1.0 were provided based on the values of the orthogonal components 1 and 2 (Figure S2).

In the roots of BDMG573\_FUS compared to the control treatment, at 0 DAT, the top three positive discriminant metabolites were  $\beta$ -alanine, mannose, and citric acid, while 4-hydroxy-proline was the most negative (Figure 6A). At 4 DAT, the three most positive metabolites were cellobiose, sorbitol, and alanine. Phenylalanine was the most negative (Figure 6B). At 8 DAT, urea, cellobiose, and sorbitol were the three most positive metabolites. Phosphoric acid was the most negative (Figure 6C). Similarly, in the roots of P1103\_FUS compared to the control treatment, at 0 DAT, the most positive discriminant metabolites were galactose, maleic acid, and alanine,

and glucuronic acid was the most negative (Figure 6D). At 4 DAT, the three most positive metabolites were the sugars galactose, sorbitol, and cellobiose. Arabinose was the most negative (Figure 6E). At 8 DAT, the three most positive metabolites were 1,3-dihydroxyacetone, adenine, and ribose. Sucrose was the most negative (Figure 6F). The variable importance of metabolites in projections (VIP scores) with  $VIP > 1.0$  were provided based on the values of the orthogonal components 1 and 2 (Figure S3).

### 3.4 | Modulation of metabolites induced by fungal co-cultivation overtime

The heatmap of the metabolite's relative abundances of shoots and roots provided an overview of the modulation by comparing treatments, genotypes, and different exposure times (Figure 7). In the shoots, two main branches have diverged the genotypes BDMG573 and P1103 (Figure 7A). Regarding the P1103 treatments, there is a branch comprising the co-cultivated and the control groups at 4 and 8 DAT in which several metabolites were increased, particularly in the co-cultivated treatments. P1103\_CNT0 was located more distant from the others. Regarding the BDMG573 treatments, the controls of the three times and BDMG573\_FUS0 were placed in the same main branch, in which it was possible to note a tendency of the decreasing of several metabolites. On the other hand, there is a branch comprising BDMG573\_FUS4 and BDMG573\_FUS8, with a tendency for the increase in several metabolites at 8 DAT.

In the roots, two main groups separated the genotypes BDMG573 and P1103, except for P1103\_FUS8, which was close to BDMG573\_FUS4 and BDMG573\_FUS8 (Figure 7B). In general, there was a similar metabolites modulation of P1103 treatments, in which there was a tendency for a decrease in the majority of metabolites in relation to BDMG573. On the other hand, two branches separated BDMG573, one comprising control treatments at 0, 4, and 8 DAT, and BDMG573\_FUS0, in which there is an increase in several metabolites. The other one, comprised of BDMG573\_FUS4, BDMG573\_FUS8, and P1103\_FUS8, presented a tendency for an increase in several other metabolites.

## 4 | DISCUSSION

### 4.1 | The rootstocks co-cultivated with FUS show different metabolic profiles

Changes in primary metabolism in vines occur in response to stressful conditions, controlled by biotic or abiotic factors (Tugizimana et al., 2018; Wong et al., 2019). Metabolomics has provided relevant information that helps understand the biochemistry of the molecular responses of plant-pathogen interactions (Chen, Ma, & Chen, 2019; Xu et al., 2015). A multivariate approach evaluated the primary metabolites profiles in the shoots and roots of the BDMG573 and P1103 *Vitis* spp. rootstock genotypes CNT and co-cultured with FUS, in vitro.

PCA showed different patterns, the metabolic profiles varied for each time, genotype, and plant organ, differences were clear for the rootstocks which indicate different responses of these genotypes against the fungus (Figures 1 and 2). It could be related to significant differences in amino acids, carbohydrates, organic acids, and other metabolites for each rootstock, highlighted in the heat maps (Figures 3 and 4). In watermelons infected with FUS, the metabolic profiles were genotype-specific and distinct which can be used to monitor the disease progress in leaves and roots (Kasote et al., 2020). Similarly, PCA was capable to differentiate the susceptible from the resistant genotype from the earliest point of *Fusarium* inoculation (Scandiani et al., 2015) or several other biotic stresses (Araújo et al., 2021; Lima et al., 2022; Oliveira et al., 2020).

At a >short time of co-culture (0 DAT), the overlapping between the BDMG573\_CNT and BDMG573\_FUS profiles in shoots demonstrates a delayed response in comparison to P1103\_FUS. It was corroborated by a high number of positive metabolites in P1103\_FUS (Figures 1 and 3A). On the other hand, roots at 0 DAT showed a similar pattern concerning overlapping areas of FUS and CNT in the PCA for both genotypes and it was also corroborated by a little number of significant metabolites of CNT and FUS comparisons (Figures 2A and 4A). There is a variety of specific responses in roots to pathogens that remains unclear (Chuberre et al., 2018). However, since roots are the first to be exposed to FUS, a possible signalling mechanism was sent from roots to shoots. It was more evident in P1103 by a quick decrease of metabolites in roots followed by a quick increase in shoots. Indeed, P1103 is an acclaimed genotype used in *Fusarium* wilt control as a rootstock for grafting varieties for wine production and beverages in Southern Brazil due its better performance (Dalbó & Feldberg, 2019). Further, previous work reported a quick increase of peptides related to defence in P1103 that may help to block the progress of infection (Vilvert et al., 2017).

At 4 DAT shoots, the profiles of the BDMG573 genotype separate from P1103 (Figure 1C), corroborated by the negative modulation of some metabolites such as citric acid, glutamine, and glyceric acid. When compared to CNT, BDMG573\_FUS also showed two different groups of positive and negative metabolites, that may be related to the progression of fungus. Otherwise, for P1103, a slight overlapping indicates much more similarities between CNT and FUS, with a positive modulation of citric acid, tyrosine, and urea (Figure 3B), that demonstrated a greater capacity to keep the shoot growing in the presence of the pathogen from medium times. Moreover, in roots at 4 DAT, the treatments BDMG573\_CNT and BDMG573\_FUS (Figure 2C) showed considerable separation of profiles and the metabolic modulation in response to the fungus attack as seen in the heat map (Figure 4B). At this time, the CNT and FUS analysis groups of the P1103 genotype both demonstrate considerable overlapping of areas (Figure 2C), denoting low metabolic modulation of the plant by the fungus in roots (Figure 6B) which favoured the metabolite accumulation in shoots, similar to short time. That is consistent with the better performance of P1103 under the progression of fungus co-cultivate times (Cavalcanti, 2021; Daldoul et al., 2020; Morsch et al., 2021).

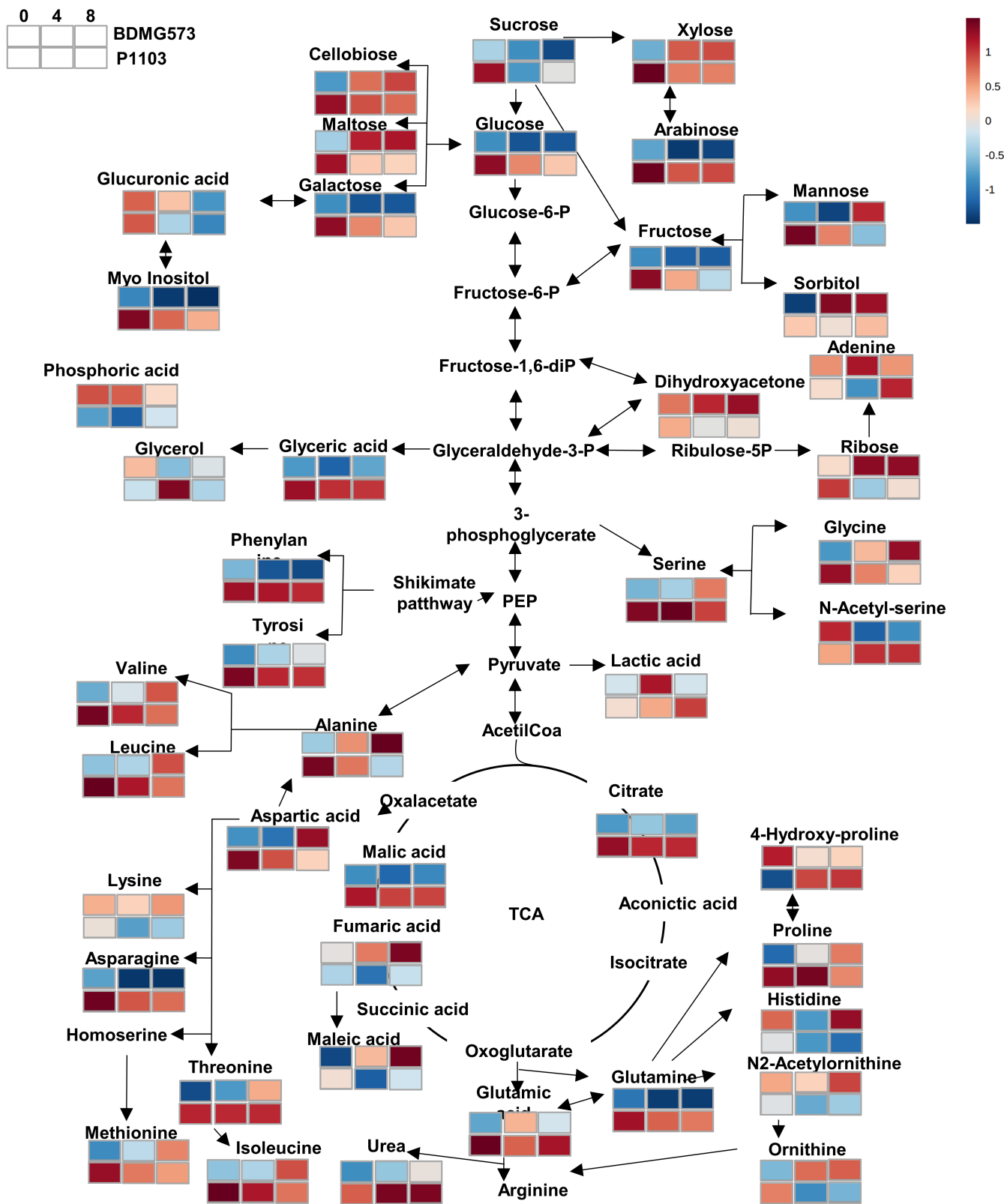


**FIGURE 8** Metabolic pathways modulated in shoots of the two varieties of *Vitis* spp. BDMG573 and P1103 co-cultivated with *Fusarium oxysporum*. The colours indicate the significant fold change of metabolites. Each square represents the log<sub>2</sub> mean of four replicates. The colour map shows an increase (red scale) or decrease (blue scale) of each metabolite in comparison to control plants. TCA, tricarboxylic acid.

In leaves at 8 DAT, PCA exhibited a complete separation of both BDMG573 and P1103 genotypes (Figure 1E), similar to 4 DAT, it may indicate that the progression of fungus impairing the plant metabolism. Indeed, it was previously reported that from 6 to 10 DAT the severity of fungus in plant growth is more pronounced in BDMG573 than P1103 (Cavalcanti, 2021). Here, it was corroborated by modulations of different metabolites for both treatments (Figure 4E). In the P1103\_FUS genotype, there was remarkable positive modulation of citric acid, added by others such as adenine, cellobiose, and sorbitol (Figure 3C). On the other hand, although BDMG573\_FUS exhibited modulation of some sugars and amino acids, such as proline and maltose, typical well-known stress markers (Ibrahim & Abdellatif, 2016; Shakirova et al., 2003), several other metabolites had a negative modulation due to fungus growth. This capacity of plants to keep positive metabolite regulation, particularly sugars, may be helpful to induce tolerance while the decrease of metabolites has a negative impact on plant response. It was corroborated by the identification of molecular markers to select and rapidly identify tolerant and sensible rootstocks to trunk diseases and abiotic stresses (Daldoul et al., 2020; Labois et al., 2020). Additionally, in roots there is an overlap between both BDMG573\_FUS, and P1103\_FUS at 8 DAT (Figure 2E), it was corroborated by the heat map that showed a similar metabolic modulation between groups (Figure 4C), in which a larger number of metabolites were changed. Therefore, it can be inferred that the roots of both genotypes have distinct responses to the pathogen attack involving different metabolites that may be potential biomarkers (Wong et al., 2020).

## 4.2 | Potential biomarkers induced by short, medium, and long times of *Fusarium* co-cultivate

The OPLS-DA models for shoots of both genotypes provided the metabolites with the highest and lowest discriminating potential for the *Fusarium* wilt of grapevine (Figure 5). In the co-cultured BDMG573 genotype (Figure 5A–C), the discriminants were the sugars ribose (at 0 DAT), 1,3-dihydroxyacetone (at 0 and 4 DAT), maltose (at 4 and 8 DAT), and sorbitol and mannose (at 8 DAT). Indeed, the increase in carbohydrates is crucial for energy metabolism maintenance and defence, which uses these metabolites as a source of carbon skeletons for several biochemical processes, including tricarboxylic acid (TCA) components for energy production (Igamberdiev & Eprintsev, 2016). Maltose stands out at the medium and late co-culture stages; it is well-reported in studies that its presence is indicative of osmotic (Darko et al., 2019) and saline stress (Shelden et al., 2016), as well as a potential biomarker of abiotic and abiotic stresses and the presence of the pathogen in the plant (Lei et al., 2016). In agreement, the increase of ribose occurs in the susceptible soybean cultivar inoculated with *Fusarium tucumaniae* (Scandiani et al., 2015), 1,3-dihydroxyacetone accumulates in heat-tolerant soybean genotypes (Chebrolu et al., 2016), the accumulation of sorbitol increases the tolerance of broccoli against pathogens by ROS scavenging (Zhang et al., 2022), as well as mannose improves the tolerance of citrus to Huanglongbing disease (Cevallos-Cevallos et al., 2012).

In the first co-cultivation time (0 DAT), shoots of the P1103 genotype presented organic acids (glyceric acid, malic acid, and citric acid) as biomarkers (Figure 5D). It is directly related to the TCA cycle to obtain energy that has great importance in the metabolic cycle of the plant (Igamberdiev & Eprintsev, 2016). Malic acid and citric acid have been related to the tolerance to abiotic stresses, such as aluminium in soybean (Sun et al., 2019; Zhou et al., 2018) and glyceric acid related to resistance to water stress (Li et al., 2019). On the other hand, in the 4 DAT of P1103\_FUS (Figure 5E), the amino acids proline, serine, and tyrosine were the main discriminants for *Fusarium* co-culture. Indeed the presence of the pathogen in the plant drives organic acids from the TCA cycle to the synthesis of amino acids (Igamberdiev & Eprintsev, 2016). Thus, proline, serine, and tyrosine are reported to increase in situations of biotic stress and could be used to produce secondary defence metabolites (Teixeira et al., 2014). Also, proline can act as an energy source, antioxidant, and osmoprotectant to stand stress conditions (Castellarin et al., 2007). The increase in proline metabolism is reported in common bean defence against *Fusarium solani* (Chen et al., 2020). For the latest day of P1103\_FUS co-culture (8 DAT), the discriminating metabolites were sorbitol, cellobiose, and urea (Figure 5F). The increased presence of carbohydrates is critical to stress response since it stabilizes proteins and protects cellular structures, such as membranes, when the stress becomes severe or persists for prolonged periods (Thalmann et al., 2016). As for the presence of urea, it seems to be related to the protein nitrogen released through catabolic reactions, the amino acids released from protein catabolism may lead to the accumulation of ammonium and urea (Beier & Kojima, 2021; Witte, 2011).

On the other hand, for roots of the BDMG573\_FUS genotype at 0 DAT, the most discriminating metabolites were  $\beta$ -alanine, mannose, and citric acid. Indeed,  $\beta$ -alanine is part of a not well-known osmoprotective and antioxidant mechanisms for plant protection against temperature, hypoxia, drought, heavy metal, and some biotic (Parthasarathy et al., 2019). Regarding mannose, it is associated with defence proteins against pathogens (dos Santos Silva et al., 2019), and tolerance in citrus (Cevallos-Cevallos et al., 2012). As the most negative discriminant, 4-hydroxy-proline stands out as an important component that reinforces against cell wall damage (Siddappa & Marathe, 2020), which may indicate root degradation by fungal enzymes (Chen, Wu, et al., 2019). Then, the roots of BDMG573\_FUS at 4 DAT, and 8 DAT, presented the cellobiose and sorbitol sugars among the main discriminants for both times (Figure 6B,C). They have been reported to be related to stress resistance and signalling the presence of disease (Meng et al., 2018; Rolland et al., 2002). Furthermore, sugars in the roots are related to the low presence of nitrogen (Zhao et al., 2020). Thus, the presence of urea in the BDMG573\_FUS of 8 DAT (Figure 6C) makes sense under prolonged biotic stress, occurring due to the high protein degradation as a nutritional source and defence signalling (Beier & Kojima, 2021; Gonçalves et al., 2020). Therefore, the OPLS-DA of the P1103 roots genotype revealed that carbohydrates were the group that showed discriminating metabolites. Carbohydrates accumulation is a common fact in plants under stresses since these compounds are strictly related to plant growth and development, providing carbon skeletons as a source of energy

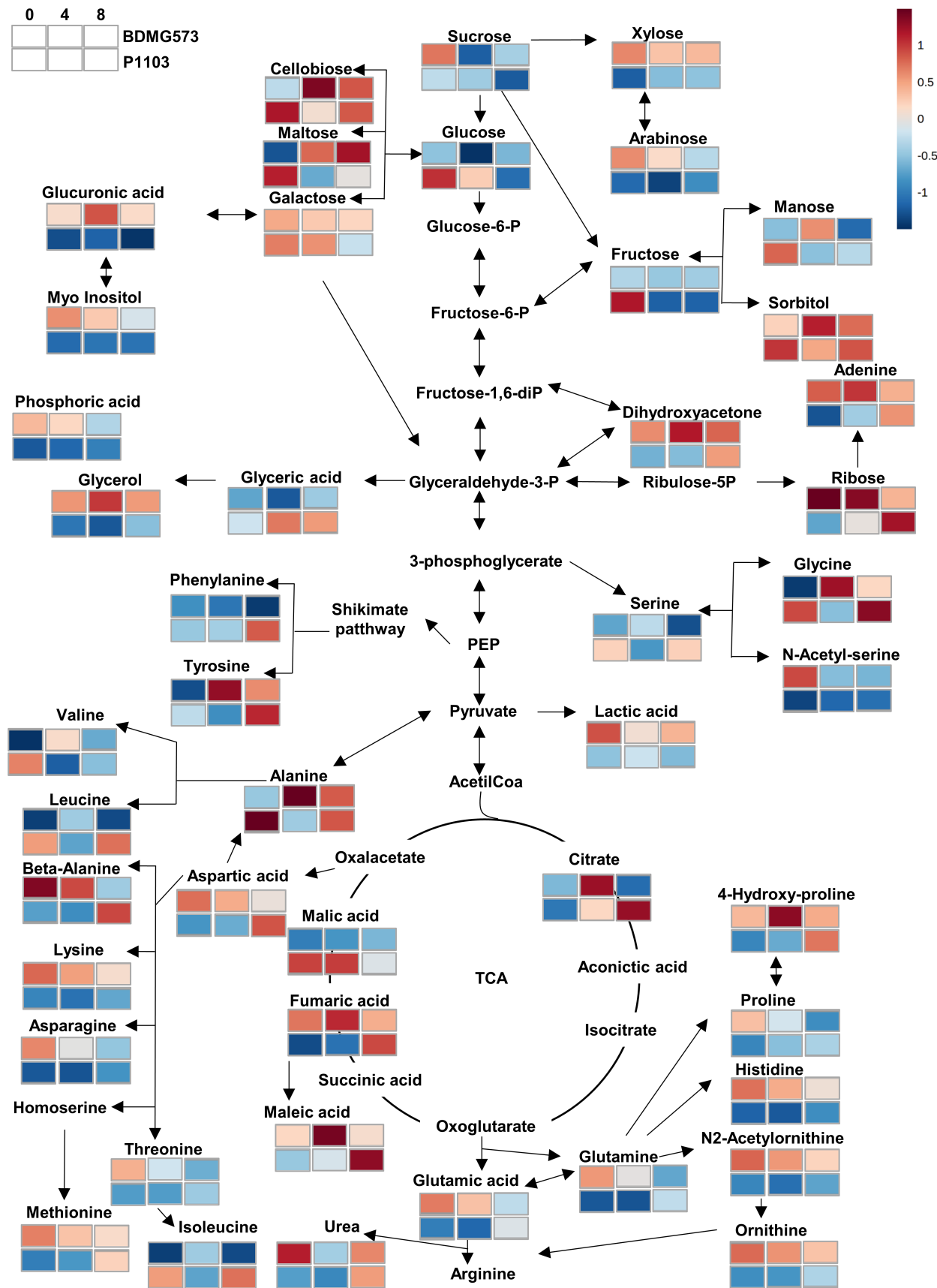


**FIGURE 9** Metabolic pathways modulated in roots of the two varieties of *Vitis* spp. BDMG573 and P1103 co-cultivated with *Fusarium oxysporum*. The colors indicate the significant fold change of metabolites. Each square represents the log<sub>2</sub> mean of four replicates. The color map shows an increase (red scale) or decrease (blue scale) of each metabolite in comparison to control plants. TCA, tricarboxylic acid.

(Lastdrager et al., 2014). In addition, they act as signalling molecules in response to stress, helping the plant survive, as discussed previously (Eveland & Jackson, 2012). At 0 DAT (Figure 6D) and 4 DAT (Figure 6E), galactose and at 8 DAT, 1,3-dihydroxyacetone (Figure 6F) have the potential of biomarkers. It reinforces that the presence of sugars in P1103 roots helps to maintain tolerance, as it is involved in the integrity of the cell wall, providing energy, and signalling in the presence of the fungus co-culture (Igamberdiev & Eprintsev, 2016; Thalmann et al., 2016).

## 5 | CONCLUSIONS

The *Vitis* spp. genotypes BDMG573 and P1103 showed distinct metabolic responses when co-cultured with *F. oxysporum* f. sp. *herbomontis*. At 4 and 8 DAT, the BDMG573\_CNT and BDMG573\_FUS groups had a greater separation of PCA areas denoting metabolic differences represented by a large number of differentially modulated metabolites. The sugar maltose was a common positive metabolite at both times of *Fusarium* co-culture, indicating a potential biomarker. Overall, in shoots glycolysis was increased since sucrose and glucose decreased, monosaccharides accumulated, and malate and citrate were drained from the TCA to keep basic levels of amino acids (Figure 8). In the roots of BDMG573 genotype, there was more similarity between the metabolic profiles at 0 DAT, and the differences were accentuated after 4 and 8 DAT increasing the number of significant positive or negative metabolites. Both cellobiose and sorbitol were common at 4 and 8 DAT demonstrating their potential as biomarkers. Thus, after 4 days of co-culture, there was a change in primary metabolism, enhancing the carbohydrates sucrose and glucose to stand against the infection. It is accentuated at 8 DAT, which leads to an increase in the number of significant amino acids related to signalling, as well as in urea related to nitrogen metabolism as a source of nutrition (Figure 9). Conversely, in the P1103 genotype, 4 and 8 DAT were similar in the shoots, and 0 and 4 DAT in the roots since there is an overlap between the CNT and FUS groups. However, the maintenance of glycolysis, TCA, and amino acids metabolism in the shoots co-cultivated with *Fusarium* was evident by the increase of primary metabolites at all times evaluated (Figure 8). It may be related to the well-known better performance of this genotype upon biotic stress. In general, the OPLS-DA projected some organic acids at (0 DAT), amino acids (4 DAT), and carbohydrates (8 DAT) in the shoots, and main sugars in the roots (at all DATs), configuring a metabolic adaptation of this genotype to abiotic and biotic stresses. Overall, this work provides significant progress in the FUS stress response of two rootstocks of *Vitis* spp. genotypes by exploring differentially modulated metabolites and potential markers for the infection over time. The data were gathered on a metabolic pathway showing glycolysis, the tricarboxylic acid cycle, and the metabolism of various amino acids. Thus, it was evident that the relationship between sugars and other metabolites to provide energy and synthesis other defence molecules still needs to be explored.

## AUTHOR CONTRIBUTIONS

Igor Rafael Sousa Costa carried out all the research, data acquisition, and wrote the manuscript. Francisco Lucas Pacheco Cavalcante and Kirley Marques Canuto helped in the metabolomics, Fábio Rossi Cavalcanti proposed the research concept. Fábio Rossi Cavalcanti, Cleber de Freitas Fernandes, and Kirley Marques Canuto contributed to co-culture experiment, Enéas Gomes-Filho and Kirley Marques Canuto revised the manuscript. Humberto Henrique de Carvalho supervised the research, data acquisition, and wrote the manuscript. All authors discussed the results and contributed to the final manuscript.

## ACKNOWLEDGMENTS

We would like to thank Embrapa Uva e Vinho for providing the *Vitis* spp. genotypes and *Fusarium* lineages and Embrapa Agroindústria Tropical to support this research. To Cryogenics Center's Physics Department of Federal University of Ceará for nitrogen supplying. To Coordenação de Aperfeiçoamento de Pessoal de Nível Superior (CAPES), Fundação Cearense de Apoio ao Desenvolvimento Científico e Tecnológico (FUNCAP), and Conselho Nacional de desenvolvimento Científico e Tecnológico (CNPq) for student's scholarship. This work was supported by Conselho Nacional de Desenvolvimento Científico e Tecnológico (CNPq), project number 408118/2021-0, and research fellowship number 306117/2022-3 and Empresa Brasileira de Pesquisa Agropecuária Project number: SEG 22.16.04.035.00.00.

## CONFLICT OF INTEREST STATEMENT

The authors declare that there is no conflicts of interest.

## DATA AVAILABILITY STATEMENT

The data that support the findings of this study are available upon request. The person responsible for distribution of material is the corresponding author.

## ORCID

Humberto Henrique de Carvalho  <https://orcid.org/0000-0001-9291-9310>

## REFERENCES

- Aalseekh, S., Aharoni, A., Brotman, Y., Contrepolis, K., D'Auria, J., Ewald, J. et al. (2021) Mass spectrometry-based metabolomics: a guide for annotation, quantification and best reporting practices. *Nature Methods*, 18, 747–756.
- Andrade, E.R., Dal Bó, M.A., Schuck, E. & Gallotti, G.J.M. (1995) Evaluation of grapevine (*Vitis* spp.) resistance to *Fusarium oxysporum* f. sp. *herbomontis* in Rio de peixe valley, Santa Catarina State, Brazil. *Acta Horticulturae*, 388, 65–70.
- Araújo, G.d.S., de Oliveira Paula-Marinho, S., de Paiva Pinheiro, S.K., de Castro Miguel, E., de Sousa Lopes, L., Camelo Marques, E. et al. (2021) H<sub>2</sub>O<sub>2</sub> priming promotes salt tolerance in maize by protecting chloroplasts ultrastructure and primary metabolites modulation. *Plant Science*, 303, 110774.
- Batista, V.C.V., Pereira, I.M.C., de Oliveira Paula-Marinho, S., Canuto, K.M., de Cássia Alves Pereira, R., Rodrigues, T.H.S. et al. (2019) Salicylic acid modulates primary and volatile metabolites to alleviate salt stress-induced photosynthesis impairment on medicinal plant *Egletes viscosa*. *Environmental and Experimental Botany*, 167, 103870.

- Beale, D.J., Pinu, F.R., Kouremenos, K.A., Poojary, M.M., Narayana, V.K., Boughton, B.A. et al. (2018) *Review of recent developments in GC-MS approaches to metabolomics-based research*. New York, NY: Springer US.
- Beier, M.P. & Kojima, S. (2021) The function of high-affinity urea transporters in nitrogen-deficient conditions. *Physiologia Plantarum*, 171, 802–808.
- Brum, M.C., Araújo, W.L., Maki, C.S. & Azevedo, J.L. (2012) Endophytic fungi from *Vitis labrusca* L. ('Niagara Rosada') and its potential for the biological control of *Fusarium oxysporum*. *Genetics and Molecular Research*, 11, 4187–4197.
- Castellarin, S.D., Pfeiffer, A., Sivilotti, P., Degan, M., Peterlunger, E. & Di Gasparo, G. (2007) Transcriptional regulation of anthocyanin biosynthesis in ripening fruits of grapevine under seasonal water deficit. *Plant, Cell and Environment*, 30, 1381–1399.
- Cavalcanti, F.R. (2021) Co-cultivo in vitro pode discriminar severidade de podridões do tronco em genótipos de videira. *Embrapa Uva e Vinho Bol Pesqui e Desenvolv online*, 20 il: 36.
- Cevallos-Cevallos, J.M., Futch, D.B., Shilts, T., Folimonova, S.Y. & Reyes-De-Corcuera, J.I. (2012) GC-MS metabolomic differentiation of selected citrus varieties with different sensitivity to citrus Huanglongbing. *Plant Physiology and Biochemistry*, 53, 69–76.
- Chebrolov, K.K., Fritschí, F.B., Ye, S., Krishnan, H.B., Smith, J.R. & Gillman, J. D. (2016) Impact of heat stress during seed development on soybean seed metabolome. *Metabolomics*, 12, 28.
- Chen, F., Ma, R. & Chen, X.-L. (2019) Advances of metabolomics in fungal pathogen-plant interactions. *Metabolites*, 9, 169.
- Chen, L., Wu, Q., He, T., Lan, J., Ding, L., Liu, T. et al. (2020) Transcriptomic and metabolomic changes triggered by *Fusarium solani* in common bean (*Phaseolus vulgaris* L.). *Genes*, 11, 177.
- Chen, L., Wu, Q., He, W., He, T., Wu, Q. & Miao, Y. (2019) Combined de novo transcriptome and metabolome analysis of common bean response to *Fusarium oxysporum* f. sp. *phaseoli* infection. *International Journal of Molecular Sciences*, 20, 6278.
- Chuberre, C., Plancot, B., Driouich, A., Moore, J.P., Bardor, M., Gügi, B. et al. (2018) Plant immunity is compartmentalized and specialized in roots. *Frontiers in Plant Science*, 9, 1–13.
- Costa, M.D., Lovato, P.E. & Sete, P.B. (2010) Micorrização e indução de quitinases e  $\beta$ -1,3-glucanases e resistência à fusariose em porta-enxerto de videira. *Pesquisa Agropecuária Brasileira*, 45, 376–383.
- Cramer, G.R. (2010) Abiotic stress and plant responses from the whole vine to the genes. *Australian Journal of Grape and Wine Research*, 16, 86–93.
- Dalbó, M.A. & Feldberg, N.P. (2019) Comportamento agrônomo de porta-enxertos de videira com resistência ao declínio de plantas jovens nas condições do estado de Santa Catarina. *Agropecuária Catarinense*, 32, 68–72.
- Daldoul, S., Boubakri, H., Gargouri, M. & Mliki, A. (2020) Recent advances in biotechnological studies on wild grapevines as valuable resistance sources for smart viticulture. *Molecular Biology Reports*, 47, 3141–3153.
- Darko, E., Végh, B., Khalil, R., Marček, T., Szalai, G., Pál, M. et al. (2019) Metabolic responses of wheat seedlings to osmotic stress induced by various osmolytes under iso-osmotic conditions. *PLoS One*, 14, 1–19.
- dos Santos Silva, P.M., de Oliveira, W.F., Albuquerque, P.B.S., dos Santos Correia, M.T. & Coelho, L.C.B.B. (2019) Insights into anti-pathogenic activities of mannose lectins. *International Journal of Biological Macromolecules*, 140, 234–244.
- Durrant, W.E. & Dong, X. (2004) Systemic acquired resistance. *Annual Review of Phytopathology*, 42, 185–209.
- Eveland, A.L. & Jackson, D.P. (2012) Sugars, signalling, and plant development. *Journal of Experimental Botany*, 63, 3367–3377.
- Feussner, I. & Polle, A. (2015) What the transcriptome does not tell—proteomics and metabolomics are closer to the plants' pathophenotype. *Current Opinion in Plant Biology*, 26, 26–31.
- Fraga, H., Santos, J.A., Malheiro, A.C., Oliveira, A.A., Moutinho-Pereira, J. & Jones, G.V. (2016) Climatic suitability of Portuguese grapevine varieties and climate change adaptation. *International Journal of Climatology*, 36, 1–12.
- Gonçalves, A.Z., Oliveira, P.M.R., Neto, A.A.C. & Mercier, H. (2020) Thinking of the leaf as a whole plant: how does N metabolism occur in a plant with foliar nutrient uptake? *Environmental and Experimental Botany*, 178, 104163.
- Grigolett-Júnior, A. & Sonego, O.R. (1993) Principais doenças fúngicas da videira no Brasil. *Circular Técnica*, 17, 36.
- Gupta, S., Chakraborti, D., Sengupta, A., Basu, D. & Das, S. (2010) Primary metabolism of chickpea is the initial target of wound inducing early sensed *Fusarium oxysporum* f. sp. *ciceri* race I. *PLoS One*, 5, e9030.
- Ibrahim, H.A. & Abdellatif, Y.M.R. (2016) Effect of maltose and trehalose on growth, yield and some biochemical components of wheat plant under water stress. *Annals of Agricultural Science*, 61, 267–274.
- Ilgamberdiev, A.U. & Eprintsev, A.T. (2016) Organic acids: the pools of fixed carbon involved in redox regulation and energy balance in higher plants. *Frontiers in Plant Science*, 7, 1–15.
- Kasote, D.M., Jayaprakasha, G.K., Singh, J., Ong, K., Crosby, K.M. & Patil, B.S. (2020) Metabolomics-based biomarkers of *Fusarium* wilt disease in watermelon plants. *Journal of Plant Diseases and Protection*, 127, 591–596.
- Labois, C., Wilhelm, K., Laloue, H., Tarnus, C., Bertsch, C., Goddard, M.L. et al. (2020) Wood metabolomic responses of wild and cultivated grapevine to infection with *Neofusicoccum parvum*, a trunk disease pathogen. *Metabolites*, 10, 1–19.
- Lagopodi, A.L., Ram, A.F.J., Lamers, G.E.M., Punt, P.J., van den Hondel, C. A.M.J.J., Lugtenberg, B.J.J. et al. (2002) Novel aspects of tomato root colonization and infection by *Fusarium oxysporum* f. sp. *radicis-lycopersici* revealed by confocal laser scanning microscopic analysis using the green fluorescent protein as a marker. *Molecular Plant-Microbe Interactions*, 15, 172–179.
- Lastdrager, J., Hanson, J. & Smeekens, S. (2014) Sugar signals and the control of plant growth and development. *Journal of Experimental Botany*, 65, 799–807.
- Lei, H., Xu, H., Feng, L., Yu, Z., Zhao, H. & Zhao, M. (2016) Fermentation performance of lager yeast in high gravity beer fermentations with different sugar supplementations. *Journal of Bioscience and Bioengineering*, 122, 583–588.
- Li, Z., Cheng, B., Yong, B., Liu, T., Peng, Y., Zhang, X. et al. (2019) Metabolomics and physiological analyses reveal  $\beta$ -sitosterol as an important plant growth regulator inducing tolerance to water stress in white clover. *Planta*, 250, 2033–2046.
- Lima, K.R.P., Cavalcante, F.L.P., Paula-Marinho, S.d.O., Pereira, I.M.C., Lopes, L.d.S., Nunes, J.V.S. et al. (2022) Metabolomic profiles exhibit the influence of endoplasmic reticulum stress on sorghum seedling growth over time. *Plant Physiology and Biochemistry*, 170, 192–205.
- Lisec, J., Schauer, N., Kopka, J., Willmitzer, L. & Fernie, A.R. (2006) Gas chromatography mass spectrometry-based metabolite profiling in plants. *Nature Protocols*, 1, 387–396.
- Meng, D., Li, C., Park, H.-J., González, J., Wang, J., Dandekar, A.M. et al. (2018) Sorbitol modulates resistance to *Alternaria alternata* by regulating the expression of an NLR resistance gene in apple. *Plant Cell*, 30, 1562–1581.
- Mondello, V., Songy, A., Battiston, E., Pinto, C., Coppin, C., Trotel-Aziz, P. et al. (2018) Grapevine trunk diseases: a review of fifteen years of trials for their control with chemicals and biocontrol agents. *Plant Disease*, 102, 1189–1217.
- Morsch, L., Somavilla, L.M., Trentin, E., Silva, K.R., de Oliveira, J.M.S., Brunetto, G. et al. (2021) Root system structure as a criterion for the selection of grapevine genotypes that are tolerant to excess copper and the ability of P to mitigate toxicity. *Plant Physiology and Biochemistry*, 171, 147–156.

- Nakabayashi, R. & Saito, K. (2015) Integrated metabolomics for abiotic stress responses in plants. *Current Opinion in Plant Biology*, 24, 10–16.
- Oliveira, D.F., Lopes, L.d.S. & Gomes-Filho, E. (2020) Metabolic changes associated with differential salt tolerance in sorghum genotypes. *Planta*, 252, 34.
- Parthasarathy, A., Savka, M.A. & Hudson, A.O. (2019) The synthesis and role of  $\beta$ -Alanine in plants. *Frontiers in Plant Science*, 10, 921.
- Reinhart, V. (2013) *Multiplicação de matrizes de porta-enxertos híbridos de videira (Vitis labrusca × Vitis rotundifolia) por micropropagação*. Dissertação (Mestrado em Ciências), Curitiba, Brasil, Universidade Federal do Paraná.
- Reveglia, P., Cinelli, T., Cimmino, A., Masi, M. & Evidente, A. (2018) The main phytotoxic metabolite produced by a strain of *Fusarium oxysporum* inducing grapevine plant declining in Italy. *Natural Product Research*, 32, 2398–2407.
- Rolland, F., Moore, B. & Sheen, J. (2002) Sugar sensing and signaling in plants. *Plant Cell*, 14, S185–S205.
- Sankaran, S., Mishra, A., Ehsani, R. & Davis, C. (2010) A review of advanced techniques for detecting plant diseases. *Computers and Electronics in Agriculture*, 72, 1–13.
- Scandiani, M.M., Luque, A.G., Razori, M.V., Ciancio Casalini, L., Aoki, T., O'Donnell, K. et al. (2015) Metabolic profiles of soybean roots during early stages of *Fusarium tucumaniae* infection. *Journal of Experimental Botany*, 66, 391–402.
- Sebastiani, M.S., Bagnaresi, P., Sestili, S., Biselli, C., Zechini, A., Orrù, L. et al. (2017) Transcriptome analysis of the Melon-*Fusarium oxysporum* f. sp. *melonis* race 1.2 pathosystem in susceptible and resistant plants. *Frontiers in Plant Science*, 8, 1–15.
- Shakirova, F.M., Sakhabutdinova, A.R., Bezrukova, M.V., Fatkhutdinova, R. A. & Fatkhutdinova, D.R. (2003) Changes in the hormonal status of wheat seedlings induced by salicylic acid and salinity. *Plant Science*, 164, 317–322.
- Shelden, M.C., Dias, D.A., Jayasinghe, N.S., Bacic, A., & Roessner, U. (2016) Root spatial metabolite profiling of two genotypes of barley (*Hordeum vulgare* L.) reveals differences in response to short-term salt stress. *Journal of Experimental Botany*, 67, 3731–3745.
- Siddappa, S. & Marathe, G.K. (2020) What we know about plant arginases? *Plant Physiology and Biochemistry*, 156, 600–610.
- Sun, X., Han, G., Meng, Z., Lin, L. & Sui, N. (2019) Roles of malic enzymes in plant development and stress responses. *Plant Signaling & Behavior*, 14, 1–8.
- Tan, K.-C., Ipcho, S.V.S., Trengove, R.D., Oliver, R.P. & Solomon, P.S. (2009) Assessing the impact of transcriptomics, proteomics and metabolomics on fungal phytopathology. *Molecular Plant Pathology*, 10, 703–715.
- Tanaka, N., Tanaka, T., Fujioka, T., Fujii, H., Mihashi, K., Shimomura, K. et al. (2001) An ellagic compound and iridoids from *Cornus capitata* root cultures. *Phytochemistry*, 57, 1287–1291.
- Teixeira, A., Martins, V., Noronha, H., Eiras-Dias, J. & Gerós, H. (2014) The first insight into the metabolite profiling of grapes from three *Vitis vinifera* L. cultivars of two controlled appellation (DOC) regions. *International Journal of Molecular Sciences*, 15, 4237–4254.
- Thalmann, M., Pazmino, D., Seung, D., Horrer, D., Nigro, A., Meier, T. et al. (2016) Regulation of leaf starch degradation by abscisic acid is important for osmotic stress tolerance in plants. *Plant Cell*, 28, 1860–1878.
- Tugizimana, F., Mhlongo, M., Piater, L. & Dubery, I. (2018) Metabolomics in plant priming research: the way forward? *International Journal of Molecular Sciences*, 19, 1759.
- Van Loon, L.C., Rep, M. & Pieterse, C.M.J. (2006) Significance of inducible defense-related proteins in infected plants. *Annual Review of Phytopathology*, 44, 135–162.
- Venkitasamy, C., Zhao, L., Zhang, R. & Pan, Z. (2019) *Grapes. Integrated processing technologies for food and agricultural by-products*. London, UK: Elsevier, pp. 133–163.
- Vilvert, E., Dalla Costa, M., Cangahuala-Inocente, G.C. & Lovato, P.E. (2017) Root proteomic analysis of grapevine rootstocks inoculated with *Rhizophagus irregularis* and *Fusarium oxysporum* f. sp. *herbomontis*. *Revista Brasileira de Ciência do Solo*, 41, 1–14.
- Volynkin, V., Vasylyk, I., Volodin, V., Grigoreva, E., Karzhaev, D., Lushchay, E. et al. (2021) The assessment of agrobiological and disease resistance traits of grapevine hybrid populations (*Vitis vinifera* L. × *Muscadinia rotundifolia* michx.) in the climatic conditions of crimea. *Plants*, 10, 1–17.
- Witte, C.P. (2011) Urea metabolism in plants. *Plant Science*, 180, 431–438.
- Wong, J.W.H., Lutz, A., Natera, S., Wang, M., Ng, V., Grigoriev, I. et al. (2019) The influence of contrasting microbial lifestyles on the pre-symbiotic metabolite responses of *Eucalyptus grandis* roots. *Frontiers in Ecology and Evolution*, 7, 1–17.
- Wong, J.W.H., Plett, K.L., Natera, S.H.A., Roessner, U., Anderson, I.C. & Plett, J.M. (2020) Comparative metabolomics implicates threitol as a fungal signal supporting colonization of *Armillaria luteobubalina* on eucalypt roots. *Plant, Cell & Environment*, 43, 374–386.
- Xu, X.-H., Wang, C., Li, S.-X., Su, Z.-Z., Zhou, H.-N., Mao, L.-J. et al. (2015) Friend or foe: differential responses of rice to invasion by mutualistic or pathogenic fungi revealed by RNAseq and metabolite profiling. *Scientific Reports*, 5, 13624.
- Zhang, L., Cenci, A., Rouard, M., Zhang, D., Wang, Y., Tang, W. et al. (2019) Transcriptomic analysis of resistant and susceptible banana corms in response to infection by *Fusarium oxysporum* f. sp. *cubense* tropical race 4. *Scientific Reports*, 9, 8199.
- Zhang, X., Zhou, H., Yao, Y., Wang, J., Gu, X., Li, B. et al. (2022) Metabolomic profiling and energy metabolism modulation unveil the mechanisms involved in enhanced disease resistance of postharvest broccoli by *Meyerozyma guilliermondii*. *Scientia Horticulturae*, 303, 111239.
- Zhao, H., Sun, S., Zhang, L., Yang, J., Wang, Z., Ma, F. et al. (2020) Carbohydrate metabolism and transport in apple roots under nitrogen deficiency. *Plant Physiology and Biochemistry*, 155, 455–463.
- Zhou, Y., Yang, Z., Xu, Y., Sun, H., Sun, Z., Lin, B. et al. (2018) Soybean NADP-malic enzyme functions in malate and citrate metabolism and contributes to their efflux under AI stress. *Frontiers in Plant Science*, 8, 1–11.
- Ziedan, E.-S.H., Embaby, E.-S.M. & Farrag, E.S. (2011) First record of *Fusarium* vascular wilt on grapevine in Egypt. *Archives of Phytopathology and Plant Protection*, 44, 1719–1727.

## SUPPORTING INFORMATION

Additional supporting information can be found online in the Supporting Information section at the end of this article.

**How to cite this article:** Costa, I.R.S., Cavalcante, F.L.P., Cavalcanti, F.R., de Freitas Fernandes, C., Gomes-Filho, E., Canuto, K.M. et al. (2023) Metabolomic exhibits different profiles and potential biomarkers of *Vitis* spp. co-cultivated with *Fusarium oxysporum* for short, medium, and long times. *Physiologia Plantarum*, 175(3), e13918. Available from: <https://doi.org/10.1111/ppl.13918>